ChemComm

Stabilizing large pores in a flexible metal–organic framework via chemical cross-linking

COMMUNICATION

Stabilizing large pores in a flexible metal–organic framework *via* chemical cross-linking

Devin S. Rollins,[a,†] Jackson Geary,[a,†] Andy H. Wong,[a] and Dianne J. Xiao[a,*]

A barrier to the isoreticular expansion of flexible metal–organic frameworks is their complex breathing behavior, which can lead to pore closure upon solvent exchange and removal. Here we show that chemical cross-linking stabilizes the open form of a flexible aluminum framework with large 17 Å pores.

Isoreticular expansion is a simple yet powerful tool for the rational design of larger pore metal–organic frameworks (MOFs).[1,2] Broadening the number of chemically robust MOFs amenable to systematic pore expansion is critical for applications requiring the encapsulation or diffusion of large guests, such as catalysis, sensing, and drug delivery.[3,4] Despite its conceptual simplicity, isoreticular expansion is often challenging to implement in practice. In addition to reduced chemical and structural stability, frameworks with large pores are prone to interpenetration, which reduces the overall accessible pore volume and surface area.[1,3,4]

Frameworks composed of rod-like secondary building units are promising candidates for isoreticular expansion, as the pore walls are tightly framed by ligands and cannot be interpenetrated.[5,6] However, rod-packing frameworks face other barriers to pore expansion, including competing phase formation and complex breathing behavior. Phase purity challenges are best illustrated by considering the reaction of a simple linker, 1,4-benzenedicarboxylic acid (H_2bdc), with various metal cations. While it is possible to achieve rod-packing motifs, such as those found in MOF-69C ($Zn_3(OH)_2(bdc)_2$)[5] and MIL-140A (ZrO(bdc)),[7] alternative phases are often equally, if not more, synthetically accessible. In the case of Zn^{2+} and Zr^{4+}, competing phases include MOF-5 ($Zn_4O(bdc)_3$)[8] and UiO-66 ($Zr_6O_4(OH)_4(bdc)_6$),[9] two of the most well-known and highly-studied frameworks to date. Because the formula units of MOF-69C vs. MOF-5 and MIL-140A vs. UiO-66 differ only in their bridging oxide/hydroxide content, achieving phase purity is nontrivial and requires the laborious testing of various solvents, additives, and heating methods.[6,10]

In contrast to the complex structural landscape observed with M^{2+} and M^{4+} salts, combining H_2bdc with a M^{3+} cation typically leads to phase-pure MIL-53(M) (M = Al, Sc, Cr, V, Fe, Ga, In) (**Fig. 1**).[11–17] However, many frameworks in the MIL-53 series display large breathing behavior, with pores opening and closing in response to environmental changes.[13] The flexibility of the MIL-53 structure type adds a new layer of difficulty to the construction of larger-pore variants, as the breathing behavior changes unpredictably as a function of linker length.[18,19] Due to these challenges, no rod-packing MOF architecture has replicated the success of the MOF-74 family (also known as $M_2(dobdc)$, $dobdc^{4–}$ = 2,5-dioxido-1,4-benzenedicarboxylate), which can be expanded to achieve permanently porous channels approaching 10 nm in diameter.[20] Broadening the
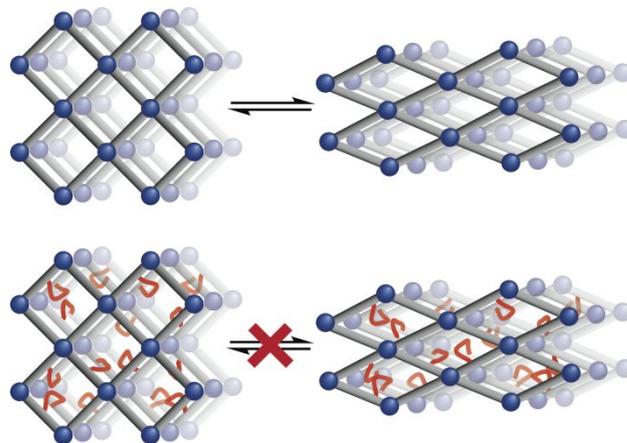

Fig. 1 | Overview of chemical cross-linking strategy to induce pore rigidification in flexible frameworks.

a. Department of Chemistry, University of Washington, Seattle, Washington 98195, United States.
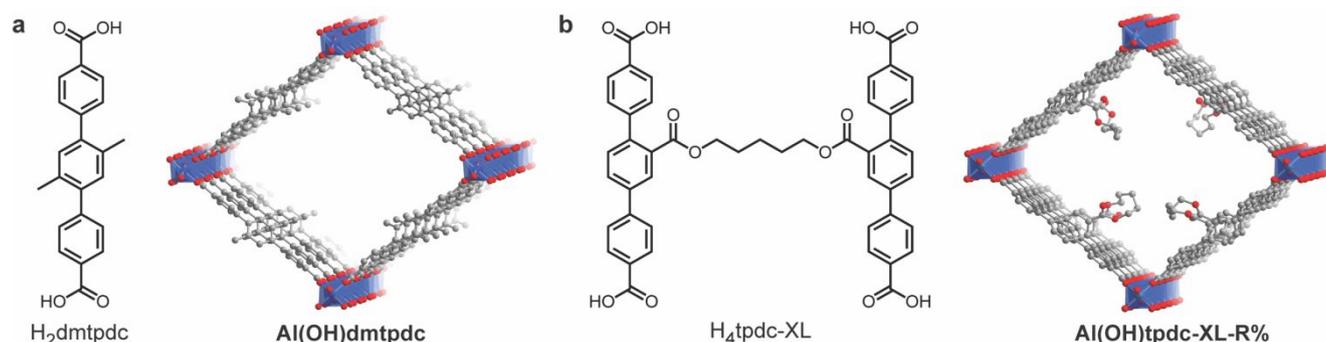† D. S. R. and J. G. contributed equally to this work.

Fig. 2 | Modeled structures of the terphenyl expanded MIL-53(Al) frameworks (a) Al(OH)dmtpdc and (b) Al(OH)tpdc-XL-R%.

number of rod-packing architectures that are robust to isoreticular expansion remains an important synthetic goal.

Here we show that chemical cross-linking can be used to enhance the structural rigidity of expanded MIL-53 analogues, providing access to large-pore variants. We report the synthesis of Al(OH)dmtpdc ($dmtpdc^{2-}$ = 2',5'-dimethyl-[1,1':4',1''-terphenyl]-4,4''-dicarboxylate), a terphenyl-expanded variant of MIL-53(Al). While Al(OH)dmtpdc partially closes upon guest evacuation, the installation of simple cross-linkers between ligands effectively locks the pores in the open form. Gas sorption measurements show that the cross-linked material possesses ~17 Å diameter pores and a Brunauer–Emmett–Teller (BET) surface area of 1870 m^2/g.

We have been interested in developing pore-expanded analogues of MIL-53(Al) due to its resistance to interpenetration, good chemical stability, and tunable pores decorated with mildly Brønsted acidic and functionalizable hydroxyl groups.[21,22] The MIL-53(Al) structure is composed of infinite chains of corner-sharing Al^{3+} octahedra bridged by bdc^{2-} ligands to form one-dimensional, diamond-shaped channels (Fig. 1). Previous reports have shown that the central benzene ring of MIL-53(Al) can be readily replaced with naphthyl, biphenyl, and bipyridyl units.[18,19] These expanded analogues are all permanently porous, with BET surface areas of 1308, 1613, and 2160 m^2/g, respectively.[18,19]

Given the apparent amenability of MIL-53(Al) to isoreticular expansion, we sought to synthesize the terphenyl variant, Al(OH)dmtpdc (2',5'-dimethyl-[1,1':4',1''-terphenyl]-4,4''-dicarboxylate) (Fig. 2). Equimolar amounts of $AlCl_3 \cdot 6H_2O$ and $H_2dmtpdc$ were heated in DMF to afford a microcrystalline white solid whose powder X-ray diffraction pattern (PXRD) largely matches the simulated pattern for fully open Al(OH)dmtpdc (Fig. 3a). However, in addition to the predicted peaks, additional features at ~6.5 and 10.5° 2ϑ were also observed. These peaks are inconsistent with the open form and are tentatively attributed to partially closed phase(s) (Fig. S5).

Like other members of the MIL-53 family, Al(OH)dmtpdc is flexible and undergoes structural changes in response to changes in solvation and pressure. While the PXRD patterns of DMF and MeCN-soaked samples are relatively similar, significant changes were observed under all other tested conditions (MeOH, THF, H_2O, vacuum activation) (Fig. S6). Specifically, the appearance of new peaks and significant peak broadening were observed. Furthermore, these structural

changes are not fully reversible, and the original PXRD pattern could not be recovered even after resolution in DMF or MeCN (Fig. S7–S8).

Gas sorption studies further confirmed that the flexible pores of Al(OH)dmtpdc are unstable to solvent exchange and activation. The theoretical surface area of fully open Al(OH)dmtpdc was calculated using the software Zeo++ and a predicted value of 3180 m^2/g was obtained.[23] In contrast, the experimentally measured BET surface area of Al(OH)dmtpdc was 645 m^2/g, significantly lower than the theoretical value, indicating substantial pore collapse upon solvent removal (Fig. 3b). To further probe the pore structure, density functional theory (DFT) methods were used to calculate the pore size distribution from 77 K N_2 adsorption data. A mixture of pore sizes was obtained, with large pores centered around 16–18 Å as well as smaller pores between 8–10 Å in diameter (Fig. S9). The broad distribution of pore diameters suggests that the activated material is not a single phase but is likely a complex mixture of open, partially open, and closed phases.

Given the structural flexibility and low porosity of Al(OH)dmtpdc, we investigated various strategies to rigidify the framework. Previous reports have shown that the presence of bulky functional groups can modulate flexible behavior through a combination of steric hindrance and intraframework interactions.[24] We hypothesized that installing short cross-linkers between pairs of ligands would more effectively stabilize the open configuration (Fig. 1). Relative to simple functional groups, cross-linkers should provide stricter geometric constraints on the motion of the pores, similar to how rigid ligands have been previously used as "girders" to enhance the mechanical stability of MOFs.[25] Cross-linking MOF ligands is well-studied, and has been used to generate "poly-MOFs" with enhanced chemical stability.[26,27] Our group has previously used short diester bridges to cross-link terphenyl expanded MOF-74 analogues.[28] Given that the MIL-53 structure type possesses similar one-dimensional pore channels, we posited an analogous approach would be viable.

We synthesized the ligand $H_4tpdc-XL$, which contains two terphenyldicarboxylic acid units linked by a 5-carbon diester chain (Fig. 2b). Combining $AlCl_3 \cdot 6H_2O$ with various ratios of $H_2dmtpdc$ and $H_4tpdc-XL$ readily produces the cross-linked framework Al(OH)tpdc-XL-R%, where 'R%' refers to the percentage of cross-linked ligand struts in the framework (Fig. 2b, see SI for synthetic details).
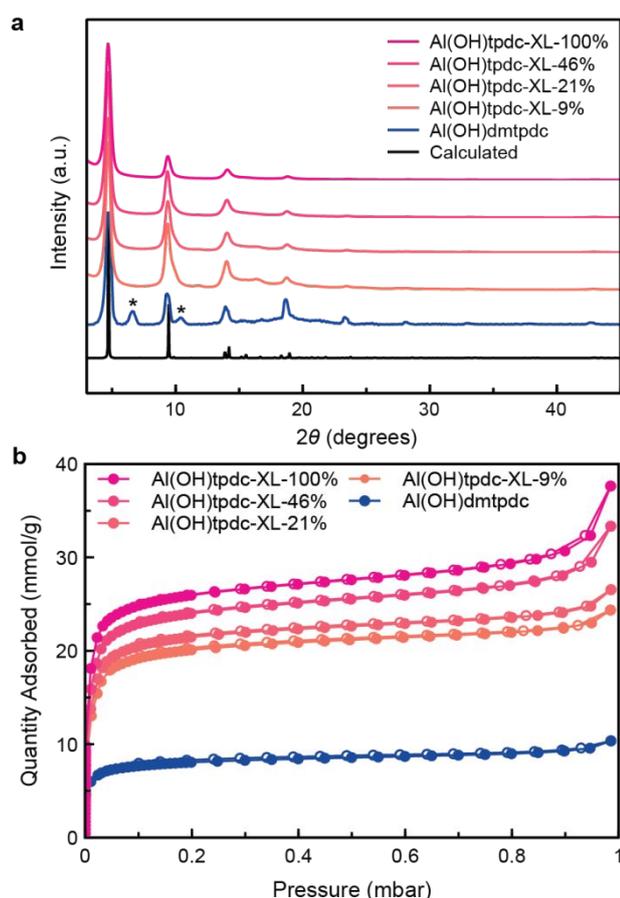
Fig. 3 | (a) PXRD patterns and (b) N₂ adsorption isotherms at 77 K for Al(OH)dmtpdc and cross-linked Al(OH)tpdc-XL-R% frameworks.

The experimental powder pattern of the cross-linked Al(OH)tpdc-XL-R% closely matches the predicted structure of a fully open Al(OH)dmtpdc framework (**Fig. 3a**). In contrast to the PXRD of Al(OH)dmtpdc, no additional peaks indicating the presence of partially closed phases were observed. Pawley refinement of the fully cross-linked material, Al(OH)tpdc-XL-100%, afforded a unit cell of a = 6.77(8) Å, b = 29.02(28) Å, and c = 24.71(22) Å in the *Pnma* space group, consistent with computational models of the fully open structure (**Fig. S10, Table S3**). ¹H NMR of digested samples confirmed the input ratio of H₂dmtpdc to H₄tpdc-XL was closely retained in the final material, with no indication of cross-linker decomposition (see SI). The incorporation of the cross-linker was further confirmed by FT-IR, with the growth of the ester carbonyl stretch at 1718 cm⁻¹ (**Fig. S11**) at higher cross-linker concentrations.

Gas sorption measurements confirm that chemically cross-linking successfully stabilizes the open configuration. A BET surface area of 1870 m²/g was obtained for the fully cross-linked Al(OH)tpdc-XL-100%, nearly three-fold higher than Al(OH)dmtpdc. While this value is still lower than the predicted value for open Al(OH)dmtpdc, a decrease in surface area is expected as the pores are partially occupied by cross-linkers. In addition to an improved surface area, the DFT pore size distribution shows only large pores centered around 16–19 Å, rather than a complex mixture of small and large pore

diameters. The slight variations in pore size between 16–19 Å may be due to subtle changes in the extent of pore opening. We found that the surface area of Al(OH)tpdc-XL-R% was directly correlated with the percentage of cross-linker incorporation. The BET surface areas increase from 1330 m²/g to 1870 m²/g between Al(OH)tpdc-XL-9% and Al(OH)tpdc-XL-100%, respectively (**Fig. 3b**).

In addition to a higher surface area, the fully cross-linked Al(OH)tpdc-XL-100% also exhibits markedly improved solvent stability compared to the parent framework. While samples immersed in protic solvents like methanol or boiling water initially lose diffraction peak intensity, the intensity is fully recovered upon re-immersion in an aprotic solvent such as acetonitrile (**Fig. S12–14**). Finally, thermogravimetric analysis of the parent and cross-linked materials reveals excellent thermal stability for the cross-linked materials (**Fig. S15**).

To probe the necessity of the crosslinker, we synthesized a simple propyl ester analogue of H₂dmtpdc, mimicking the steric profile of the cross-linked ligand but with greater rotational freedom (**Fig. S16**). The resultant propyl ester-functionalized framework shows poor crystallinity compared to both Al(OH)dmtpdc and Al(OH)tpdc-XL-100%, and a BET surface area of only 1275 m2/g (**Fig. S17-S18**). Together, these results suggest that the rigidity engendered by cross-linkers plays a crucial role in stabilizing open pores.

Next, the configuration of the cross-linkers in the pores was probed via modeling studies. We investigated two possible configurations, which are illustrated in **Fig. 4**. In the "down-pore" configuration, the cross-linker bridges adjacent ligands down the pore channel, whereas in the "across-pore" configuration, the cross-linker bridges neighboring ligands in the *bc* plane. To carry out these calculations, the extended structure of Al(OH)dmtpdc was first optimized in Materials Studio (**Table S3**) and then truncated to two neighboring ligands. The ligands were partially frozen such that only the central phenyl rings could freely move, mimicking the geometric restrictions of the framework lattice. For both configurations, a bridging cross-linker was added, and the geometries were optimized using DFT (see SI for computational details). Altogether, our modeling studies suggest the "down-pore"
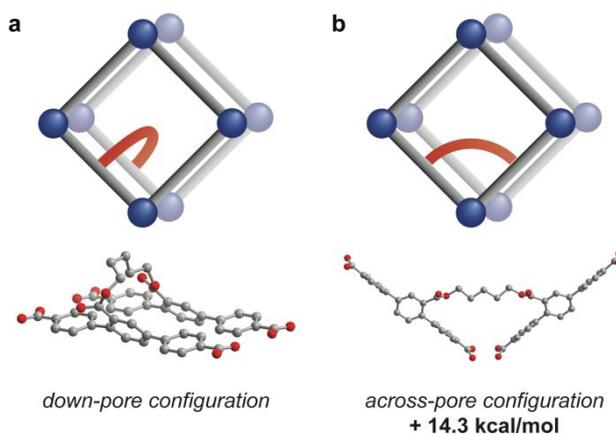

Fig. 4 | Truncated model structures showing the (a) "down-pore" and (b) "across-pore" crosslinker configurations.

configuration is the dominant structure in the framework, with an energetic preference of over 14 kcal/mol (**Table S3**).

Due to its increased pore size and structural stability, we hypothesized that the fully cross-linked Al(OH)tpdc-XL-100% would outperform Al(OH)dmtpdc in applications requiring the diffusion of guests through the pores, such as catalysis. The Prins condensation between β-pinene and paraformaldehyde to form nopol was investigated as a proof-of-concept reaction (see **Scheme S3** for reaction overview). Previous reports have shown that the Prins reaction can be catalyzed by Lewis acidic metal centers in MOFs.[29] While the bulk of Al^{3+} centers in MIL-53(Al) are coordinatively saturated, the framework is known to contain a small amount of Lewis acidic defect sites that can be used to catalyze this reaction.[30] We found that cross-linked Al(OH)tpdc-Xl-100% outperformed the noncross-linked framework. Specifically, Al(OH)dmtpdc showed negligible catalytic activity at 80 °C in MeCN, while Al(OH)tpdc-XL-100% showed ca. 19 % conversion under the same conditions (**Table S7**). We note that the incomplete conversion may be due to the relatively low concentration of Lewis acidic defect sites as well as possible product adsorption and inhibition.

In conclusion, we have shown how cross-linking stabilizes open pores in the terphenyl expanded analogues of MIL-53(Al), leading to improved mass transport and higher catalytic activity. While we have focused on the MIL-53 family, chemical cross-linking may serve as a generalizable route for accessing stable, large-pore variants of flexible metal–organic frameworks.

Conflicts of interest

There are no conflicts to declare.

Notes and references

1   M. Eddaoudi, J. Kim, N. Rosi, D. Vodak, J. Wachter, M. O'Keeffe and O. M. Yaghi, *Science*, 2002, **295**, 469–472.
2   O. M. Yaghi, M. O'Keeffe, N. W. Ockwig, H. K. Chae, M. Eddaoudi and J. Kim, *Nature*, 2003, **423**, 705–714.
3   L. Song, J. Zhang, L. Sun, F. Xu, F. Li, H. Zhang, X. Si, C. Jiao, Z. Li, S. Liu, Y. Liu, H. Zhou, D. Sun, Y. Du, Z. Cao and Z. Gabelica, *Energy Environ. Sci.*, 2012, **5**, 7508.
4   W. Xuan, C. Zhu, Y. Liu and Y. Cui, *Chem. Soc. Rev.*, 2012, **41**, 1677–1695.
5   N. L. Rosi, J. Kim, M. Eddaoudi, B. Chen, M. O'Keeffe and O. M. Yaghi, *J. Am. Chem. Soc.*, 2005, **127**, 1504–1518.
6   N. L. Rosi, M. Eddaoudi, J. Kim, M. O'Keeffe and O. M. Yaghi, *Angew. Chem. Int. Ed.*, 2002, **41**, 284.
7   V. Guillerm, F. Ragon, M. Dan-Hardi, T. Devic, M. Vishnuvarthan, B. Campo, A. Vimont, G. Clet, Q. Yang, G. Maurin, G. Férey, A. Vittadini, S. Gross and C. Serre, *Angew. Chem. Int. Ed.*, 2012, **51**, 9267–9271.
8   H. Li, M. Eddaoudi, M. O'Keeffe and O. M. Yaghi, *Nature*, 1999, **402**, 276–279.
9   J. H. Cavka, S. Jakobsen, U. Olsbye, N. Guillou, C. Lamberti, S. Bordiga and K. P. Lillerud, *J. Am. Chem. Soc.*, 2008, **130**, 13850–13851.
10 W. Liang, R. Babarao and D. M. D'Alessandro, *Inorg. Chem.*, 2013, **52**, 12878–12880.
11 C. Serre, F. Millange, C. Thouvenot, M. Noguès, G. Marsolier, D. Louër and G. Férey, *J. Am. Chem. Soc.*, 2002, **124**, 13519–13526.
12 K. Barthelet, J. Marrot, D. Riou and G. Férey, *Angewandte Chemie International Edition*, 2002, **41**, 281–284.
13 T. Loiseau, C. Serre, C. Huguenard, G. Fink, F. Taulelle, M. Henry, T. Bataille and G. Férey, *Chemistry – A European Journal*, 2004, **10**, 1373–1382.
14 T. R. Whitfield, X. Wang, L. Liu and A. J. Jacobson, *Solid State Sciences*, 2005, **7**, 1096–1103.
15 E. V. Anokhina, M. Vougo-Zanda, X. Wang and A. J. Jacobson, *J. Am. Chem. Soc.*, 2005, **127**, 15000–15001.
16 M. Vougo-Zanda, J. Huang, E. Anokhina, X. Wang and A. J. Jacobson, *Inorg. Chem.*, 2008, **47**, 11535–11542.
17 J. P. S. Mowat, S. R. Miller, A. M. Z. Slawin, V. R. Seymour, S. E. Ashbrook and P. A. Wright, *Microporous and Mesoporous Materials*, 2011, **142**, 322–333.
18 I. Senkovska, F. Hoffmann, M. Fröba, J. Getzschmann, W. Böhlmann and S. Kaskel, *Microporous and Mesoporous Materials*, 2009, **122**, 93–98.
19 E. D. Bloch, D. Britt, C. Lee, C. J. Doonan, F. J. Uribe-Romo, H. Furukawa, J. R. Long and O. M. Yaghi, *Journal of the American Chemical Society*, 2010, **132**, 14382–14384.
20 H. Deng, S. Grunder, K. E. Cordova, C. Valente, H. Furukawa, M. Hmadeh, F. Gandara, A. C. Whalley, Z. Liu, S. Asahina, H. Kazumori, M. O'Keeffe, O. Terasaki, J. F. Stoddart and O. M. Yaghi, *Science*, 2012, **336**, 1018–1023.
21 M. Meilikhov, K. Yusenko and R. A. Fischer, *J. Am. Chem. Soc.*, 2009, **131**, 9644–9645.
22 U. Ravon, G. Chaplais, C. Chizallet, B. Seyyedi, F. Bonino, S. Bordiga, N. Bats and D. Farrusseng, *ChemCatChem*, 2010, **2**, 1235–1238.
23 T. F. Willems, C. H. Rycroft, M. Kazi, J. C. Meza and M. Haranczyk, *Microporous and Mesoporous Materials*, 2012, **149**, 134–141.
24 S. Henke, A. Schneemann, A. Wütscher and R. A. Fischer, *J. Am. Chem. Soc.*, 2012, **134**, 9464–9474.
25 E. A. Kapustin, S. Lee, A. S. Alshammari and O. M. Yaghi, *ACS Cent. Sci.*, 2017, **3**, 662–667.
26 C. A. Allen, J. A. Boissonnault, J. Cirera, R. Gulland, F. Paesani and S. M. Cohen, *Chemical Communications*, 2013, **49**, 3200.
27 Z. Zhang, H. T. H. Nguyen, S. A. Miller and S. M. Cohen, *Angewandte Chemie International Edition*, 2015, **54**, 6152–6157.
28 J. Geary, A. H. Wong and D. J. Xiao, *J. Am. Chem. Soc.*, 2021, **143**, 10317–10323.
29 M. Opanasenko, A. Dhakshinamoorthy, Y. K. Hwang, J.-S. Chang, H. Garcia and J. Čejka, *ChemSusChem*, 2013, **6**, 865–871.
30 Z. Wang, M. Babucci, Y. Zhang, Y. Wen, L. Peng, B. Yang, B. C. Gates and D. Yang, *ACS Appl. Mater. Interfaces*, 2020, **12**, 53537–53546.